

# Chapter 2

## From laminar to turbulent flows

Turbulent flows can often be observed to arise from laminar flows as the Reynolds number is increased<sup>1</sup>. The transition to turbulence happens because small disturbances to the flow are no longer damped by the flow, but begin to grow by taking energy from the original laminar flow. This natural process is easily visualized by watching the simple stream of water from a faucet (or even a pitcher). Turn the flow on very slow (or pour) so the stream is very smooth initially, at least near the outlet. Now slowly open the faucet (or pour faster) and observe what happens, first far away, then closer to the spout. The surface begins to exhibit waves or ripples which appear to grow downstream. In fact, they are growing by extracting energy from the primary flow. Eventually they grow enough that the flow breaks into drops. These are capillary instabilities arising from surface tension, but regardless of the type of instability, the idea is the same – infinitesimal disturbances have grown to disrupt the simplicity of the laminar flow. In this lecture we investigate how this transition from laminar to turbulent dynamics occurs.

Laminar flows are solutions of the Navier-Stokes equations in the limit when nonlinearities can be neglected. This situation corresponds to the Stokes approximation; the flow is given by a balance between external forcing (mechanical or thermodynamical) and dissipation. The corresponding velocity field is entirely predictable and has the same regularity properties as the applied external forces.

As the Reynolds number is increased, nonlinearities are no longer negligible. There is a critical Reynolds number, above which the system bifurcates toward completely new solutions. These solutions correspond to breaking of symmetries of the original flow. For example a steady flow submitted to time independent forcing becomes time periodic. Usually the state resulting from a first bifurcation is still very regular.

---

<sup>1</sup>In this lecture Reynolds number is used to identify whatever nondimensional number is appropriate to characterize the onset of turbulence in the problem at hand.

When the Reynolds number is increased even further, the flow that emerged after the primary bifurcation can itself become unstable to new modes breaking new symmetries. The set of bifurcation continues until the global dynamics of the flow becomes very complicated, i.e. turbulent.

The transition from simple to complex behavior is observed in models as simple as deterministic maps. Thus in the next section we derive a map based on a loose analogy to the Navier-Stokes equation. A study of solutions of the map will provide an introduction to the problem of the onset of complexity and chaos in simple deterministic systems. These results will provide an introduction to the problem of onset of turbulence. How can irregular and apparently stochastic solutions appear in fluid flows that are governed by deterministic equations?

## 2.1 The logistic map as a poor man's Navier-Stokes equation

Following Frisch we introduce a discrete map that mimics some of the properties of the Navier-Stokes equations. A sort of a poor man's Navier-Stokes equation. We begin with the incompressible form of the Navier-Stokes equations,

$$\mathbf{u}_t + \mathbf{u} \cdot \nabla \mathbf{u} = -\nabla p + Re^{-1} \nabla^2 \mathbf{u} + \mathbf{F}, \quad (2.1)$$

$$\nabla \cdot \mathbf{u} = 0. \quad (2.2)$$

We now express the solutions in terms of the Fourier representation of  $\mathbf{u}$ ,

$$\mathbf{u}(\mathbf{x}, t) = \sum_i a_i(t) e^{i\mathbf{k} \cdot \mathbf{x}}. \quad (2.3)$$

This resulting infinite system of ordinary differential equations (ODEs) for the Fourier coefficients is known as a Galerkin projection of the Navier-Stokes equations; e.g.,

$$\dot{a}_i = - \sum_{jk} A_{ijk} a_j a_k - Re^{-1} |\mathbf{k}|^2 a_i + F_i. \quad (2.4)$$

Equation (2.4) is simple to understand. Every mode  $a_i$  represents a component of the velocity field with a lengthscale  $|\mathbf{k}|$ . The velocity field at each lengthscale can be changed through nonlinear interaction with other modes, through linear damping or through forcing  $F_i$ . The nonlinear interaction are quadratic and their strength is controlled by the coefficients  $A_{ijk}$ . Damping is inversely proportional to the lengthscale and thus it is more efficient for small-scale modes. A detailed derivation of equation (2.4) is given in chapter 3 of Salmon's book.

In order to keep the problem simple let us remove all but a single arbitrary wave mode. This procedure is called a Galerkin truncation. This results in an equation of

the form,

$$\dot{a} = -Aa^2 - Re^{-1}|\mathbf{k}|^2 a, \quad (2.5)$$

i.e. an evolution equation for one mode forced by a quadratic nonlinearity and damping. This derivation is not formally correct. A careful expansion of the Navier-Stokes equation would show that a mode cannot interact nonlinearly with itself. In other words  $A_{iii} = 0$ . We ignore the issue for the moment. The only justification for equation (2.5) is that it has a quadratic nonlinearity and dissipation, much alike the Navier-Stokes equation and it might be a useful paradigm to study the onset of complex behavior in a simple deterministic system.

It is straightforward to solve (2.5) numerically. Here we will employ a simple forward Euler single-step, explicit time integration procedure. This leads to,

$$\frac{a_{n+1} - a_n}{\tau} = -Aa_n^2 - Re^{-1}|\mathbf{k}|^2 a_n, \quad (2.6)$$

where  $\tau$  is an arbitrary discrete time step parameter. We now rearrange the equation as,

$$a_{n+1} = \tau A a_n \left( \frac{1 - Re^{-1}\tau|\mathbf{k}|^2}{\tau A} - a_n \right). \quad (2.7)$$

This map can be reduced to a well studied example, if we require,

$$\frac{1 - Re^{-1}\tau|\mathbf{k}|^2}{\tau A} = 1, \quad (2.8)$$

which implies that,

$$\tau A = (1 - Re^{-1}\tau|\mathbf{k}|^2). \quad (2.9)$$

This in turn permits us to write (2.6) as,

$$a_{n+1} = 4 \left(1 - Re^{-1}\tau|\mathbf{k}|^2\right) a_n (1 - a_n) = r a_n (1 - a_n), \quad (2.10)$$

which is the well known logistic map.

It is easily seen that as  $Re \rightarrow \infty$ ,  $r \rightarrow 1$  from below. Since  $a(1 - a)$  has a maximum at  $1/4$  for  $a \in [0,1]$  we see that we should rescale  $r$  by a factor of 4 to obtain that the range of values for  $r$  is between zero and four, just as in the logistic map. It is also worth observing that  $r$  depends on the wavevector magnitude, and on the numerical time step parameter. In particular, we see that the product of these factors must be less than  $Re$  in order for  $r > 0$  to hold. This implies that as the wavevector magnitude increases, the time step size must decrease, just as would certainly be the case in order to maintain stability of an explicit time-stepping method such as forward Euler.

We will show that the logistic map displays broadband spectrum in time, nonlinearity, unpredictable behavior, and time reversibility. However it is derived assuming a single lengthscale and it cannot display any spatial structure. Thus the logistic map is poor man's Navier-Stokes equation and cannot display turbulent behavior. However it is a useful tool to study how a deterministic system can produce chaos and unpredictable behavior.

### 2.1.1 Linear solutions of the logistic map

We start by studying linear solutions of the logistic map. The variable  $a_n$  represents the amplitude of the velocity at time  $n\tau$ . For convenience we will now switch from  $a_n$  to  $x_n$  to indicate the mode amplitude. The logistic map is a one dimensional map of the form  $x_{n+1} = F(x_n)$ ,

$$x_{n+1} = rx_n(1 - x_n). \quad (2.11)$$

The iteration of one dimensional maps is easy to see graphically: if we plot  $y = F(x)$  and  $y = x$ , the iterations are given by successive steps between these two curves,

$$y = F(x_n), \quad x_{n+1} = y. \quad (2.12)$$

Successive iterations from a given initial values are given by successive operations of the map  $F$ , an operation known as functional composition,

$$x_1 = F(x_0), \quad (2.13)$$

$$x_2 = F(x_1) = F(F(x_0)), \quad (2.14)$$

$$\vdots \quad (2.15)$$

$$x_n = F(x_{n-1}) = F(F \dots F(x_0)). \quad (2.16)$$

We use the matlab function `cobweb.m` to study the properties of the map. The intersection  $x_f$  of  $y = F(x)$  with  $y = x$  is a fixed point of the iteration, if,

$$F(x_f) = x_f. \quad (2.17)$$

We can easily answer the question of whether an initial condition close to  $x_f$  approaches the fixed point under iteration (when we call the fixed point stable) or moves away from it (unstable fixed point) by linearizing the evolution about  $x_f$ : write  $x = x_f + \delta x$  and then using a Taylor expansion with  $F'(x)$  the derivative of the function,

$$x_{n+1} = x_f + \delta x_{n+1} = F(x_f + \delta x_n) \approx F(x_f) + \delta x_n F'(x_f) \quad (2.18)$$

so that

$$\delta x_{n+1} = F'(x_f) \delta x_n \quad (2.19)$$

and  $|\delta x_n|$  will increase on successive iterations for  $F'(x_f) > 1$ . Thus the fixed point is stable for  $F'(x_f) < 1$  and is unstable for  $F'(x_f) > 1$ . This procedure is the map equivalent of the linear stability analysis of solutions of the Navier-Stokes equations. In 12.803 we considered the linear stability analysis of shear flows. In that case we considered the stability as a function of external parameters like the shear and its curvature. Here we will study the stability of fixed points for different Reynolds numbers.

### 2.1.2 Bifurcations and the onset of chaos in the logistic map

In the logistic map for small values of  $r$  there is only one stable fixed point  $x_f$  and almost all initial conditions lead to an orbit that converges to the fixed point ( $x = 0$  and  $x = 1$  being exceptional initial conditions). These solutions correspond to the laminar flows at small Reynolds numbers. Nonlinearities are subdominant. However things change as we increase  $r$ . What happens when  $x_f$  becomes unstable (which happens at  $r = 3$ )?

#### The first bifurcation

As the map parameter  $r$  is changed, the character of the long time solution dramatically changes, from a fixed point to a time dependent solution. These changes are called bifurcations. For values of  $r$  slightly larger than 3, the solution converges to an orbit which alternately visits two values  $x_1$  and  $x_2$ : this is the discrete time version of a limit cycle or periodic orbit (here period two). The second iterate function  $y = F^2$  yields three intersections with the line  $y = x$ . It is easy to check that at two of these the magnitude of the slope  $|dF^2/dx|$  is less than unity, i.e. there are two stable fixed points of  $F^2$ , and these correspond to  $x_1$  and  $x_2$ . The third fixed point of  $F^2$  is unstable:  $x_f$  is of course an unstable fixed point of  $F$ . These issues are illustrated by the matlab functions `cobweb.m` and `logistic_fp.m`. Try to run them using  $r = 3.2$ .

#### The second bifurcation

Set  $r$  to  $r = 3.5$  and look at the iterations of  $F$ . The period two orbit has gone unstable, and the trajectory converges to a period four orbit. We have seen that the period two orbit is simple (a fixed point!) in  $F^2$ . We can understand the second bifurcation by studying the fixed points of  $F^4$ . The instability of the period two orbit is seen to be associated with the slope of  $F^4$  becoming greater than unity, and again two new fixed points of  $F^4$  develop.

#### Further bifurcations

The analysis of bifurcations gets more and more awkward as  $r$  increases. Hence we switch to numerical exploration. But keep in mind that numerics can find attractors

but miss the unstable structures. With  $r$  slightly bigger than 3.54, the population will oscillate between 8 values, then 16, 32, etc. The lengths of the parameter intervals which yield the same number of oscillations decrease rapidly; the ratio between the lengths of two successive such bifurcation intervals approaches the Feigenbaum constant,

$$\delta = \lim_{n \rightarrow \infty} \frac{r_n - r_{n-1}}{r_{n+1} - r_n} = 4.669 \dots \quad (2.20)$$

All of these behaviors do not depend on the initial population. This is the so-called period-doubling bifurcation.

The bifurcations that occur, and the different types of orbits, are well shown by the bifurcation map. This is constructed with the parameter  $r$  along the abscissa, and all values of  $x$  visited (after some numbers of iterations to eliminate transients) plotted as points along the ordinate. A fixed point orbit over a range of  $r$  appears as a single curve, which splits into two curves at the bifurcation to the period two orbit etc. Chaotic dynamics, where the orbit visits an infinite number of points (otherwise the orbit would repeat, and therefore be periodic) appears as bands of continua of points (subject to limitations of how many points are actually plotted in the implementation).

The bifurcation diagram of the logistic map shows that simple systems can have an amazingly rich bifurcation structure. This complexity in the logistic map was first studied by May in the context of population dynamics. You can create a bifurcation map with the matlab function `logistic_bif.m`.

### The onset of chaos

At  $r = 3.569946 \dots$  the orbits become very irregular and we can no longer see any oscillations. Slight variations in the initial population yield dramatically different results over time. These are signatures that the orbits have become chaotic. Notice, however, that periodic windows mysteriously appear here and there as we further increase  $r$ . These are sometimes called *islands of stability*. The largest window is near (3.8284, 3.8415) where there is a period three orbit. For slightly higher values of  $r$  oscillations flicker between 6 values, then 12 etc. There are other ranges which yield oscillation between 5 values etc.; all oscillation periods do occur. These behaviours are again independent of the initial value.

At  $r = 4$ , the large admissible value for  $r$ , the map is fully chaotic. The iterations appear completely random, and the values eventually fill up the whole interval  $[0, 1]$ . This chaotic motion can be completely understood by making a transformation of variables. Define,

$$x_n = \sin^2(\pi z_n/2). \quad (2.21)$$

Figure removed due to copyright restrictions.

Figure 2.1: The complete orbit diagram, which is the plot of the map's attractor as a function of  $r$ . This amazing diagram is as beautiful as it is mysterious. If you look at it more closely, you will find that lying just above the periodic windows in the chaotic region are small copies of the whole orbit diagram. Thus this picture has fine structures at arbitrarily small scales.

The iteration of  $z$  for  $r = 4$  is then just,

$$z_{n+1} = \begin{cases} 2z_n, & 0 \leq z_n \leq 1/2 \\ 2 - 2z_n, & 1/2 \leq z_n \leq 1 \end{cases} \quad (2.22)$$

This is known as the tent map. Successive values of  $z_n$  from a random initial value are as random as a coin toss (and in fact in binary representation answering the question of whether the  $n$ -th value is to the right or left of 0.5 just gives the binary representation of the initial value, which is random for a random initial value). Beyond  $r = 4$ , the values eventually leave the interval  $[0, 1]$  and diverge for almost all initial values.

It is interesting to consider the temporal spectrum of orbits of the logistic map for different values of  $r$ . At the appearance of the period two orbit, the spectrum has a single peak at  $f = 1/2$ . As  $r$  increases, period doubling bifurcations generate new peaks at sub-harmonics  $f/2$ ,  $f/4$  and so on. Notice that the appearance of sub-harmonics is quite different from the appearance of super-harmonics ( $2f$ ,  $4f$ , ...) as a result of quadratic nonlinearities. Finally, at the onset of chaos the number of excited harmonics becomes large and the spectrum appears to be broadband.

## 2.2 Chaos and sensitivity to initial conditions

The orbits of the logistic map become very erratic when  $r = 4$ . But what do we mean by the orbits being chaotic? The onset of chaos is defined by a "sensitive dependence on initial conditions", i.e. orbits with similar initial conditions diverge exponentially fast. The sensitive dependence on initial conditions can be made quantitative by generalizing the idea of instability of a fixed point. Equation (2.19) can in fact be used for the expansion of a small separation at any  $x_n$ ,

$$\delta x_{n+1} = F'(x_n)\delta x_n, \quad (2.23)$$

so that the product of the derivatives at successive iterations gives us the expansion (or contraction) of the separation between the iterates of nearby points.

More precisely we start with initial conditions  $x_0$  and  $x_0 + \Delta x$  and ask for the distance between the  $n$ -th iterates, which we expect to grow as,

$$|\delta x_n| = \Delta x e^{n\lambda(x_0)}, \quad (2.24)$$

where  $\lambda(x_0)$  is the so-called *Lyapunov exponent* for the initial condition  $x_0$ , i.e.

$$\lambda(x_0) = \lim_{n \rightarrow \infty} \lim_{\Delta x \rightarrow 0} \frac{1}{n} \log \left| \frac{F^n(x_0 + \Delta x) - F^n(x_0)}{\Delta x} \right| = \lim_{n \rightarrow \infty} \frac{1}{n} \log \left| \frac{dF^n(x_0)}{dx_0} \right|. \quad (2.25)$$

For systems like the logistic map for  $r = 4$  the limit exists and is independent of the initial condition  $x_0$  for almost all initial conditions (e.g. not those points exactly on

unstable periodic orbits), and will be denoted  $\lambda$  and called the Lyapunov exponent of the map. The derivative can be evaluated by the chain rule in terms of derivatives of  $F$  at the intermediate iterations,

$$\frac{dF^n(x_0)}{dx_0} = F'(x_{n-1})F'(x_{n-2}) \dots F'(x_1)F'(x_0). \quad (2.26)$$

Thus we can compactly write,

$$\lambda = \langle \log |F'| \rangle, \quad (2.27)$$

where the average  $\langle \rangle$  is over the iterations of the map. A positive value of  $\lambda$  corresponds to the difference between closely spaced initial conditions growing (on average exponentially) with iteration i.e. to sensitive dependence on initial conditions. Thus a positive Lyapunov exponent is a signature of chaos, and may be used as a defining criterion. The Lyapunov exponents of the logistic map are shown as a function of  $r$  in figure 2.2. Positive values of  $\lambda$  appear for larger values of  $r$ . The occasional negative dips correspond to the islands of stability.

| $r$            | $\lambda$            | Comments                       |
|----------------|----------------------|--------------------------------|
| 1              | $0 - 0.005112 \dots$ | start stable fixed point       |
| 3              | $-0.003518 \dots$    | start stable 2-cycle           |
| 3.449489743... | $-0.003150 \dots$    | start stable 4-cycle           |
| 3.56994571869  | $+0.001934 \dots$    | start of chaos (Dewdney, 1988) |
| 3.828427125... | $-0.003860 \dots$    | start stable 3-cycle           |
| 3.9            | $+0.7095 \dots$      | back into chaos                |
| 4              | $+0.6931 \dots$      | end of chaos                   |

(2.28)

## 2.3 Routes to chaos

The logistic map is a useful example to study the onset of chaos in a deterministic system as a function of an external parameter like the Reynolds number  $r$ . The question arises as to whether the bifurcation patterns that leads to the onset of chaos is typical of other systems, or whether it is an oddity of the logistic map. For the moment we restrict the discussion to maps and low order dynamical systems (i.e. systems described by a small number of ordinary differential equations). We will extend the discussion to turbulent flows at the end of the lecture.

Despite the richness and complexity in the orbits generated by maps and dynamical systems, it turns out that the routes to chaos are quite universal and can be broadly grouped in three classes: the period doubling route, the intermittency route, and the quasi-periodic route. The logistic map is an example of a map that follows the first route.

Figure removed due to copyright restrictions.

Figure 2.2: The bifurcation diagram together with the corresponding Lyapunov exponents for the logistic map.

### **Period doubling route (Feigenbaum, 1978)**

The system loses stability through period-doubling, pitchfork bifurcations. The system undergoes a cascade of such period-doublings until at the accumulation point one observes aperiodic behaviour, but no broad-band spectrum. Note also, that if one has seen three bifurcations, a fourth bifurcation becomes more probable than a third after only two, etc. This route to chaotic behavior has been observed in heat transport by convection.

### **Intermittency route (Pomeau & Maneville, 1980)**

The system loses stability through intermittency, i.e. chaos appears intermittently within an otherwise regular trajectory. There are no clear cut precursors for this route although it is characterized by long periods of periodic motion with bursts of chaos. The logistic map shows transition to chaos through intermittency for  $r = 3.8282$  just below the period three window. Intermittent behavior generally happens close to a saddle-node bifurcation.

### **Quasi-periodic route (Ruelle & Takens, 1971)**

In this route to chaos, there are a number of periodic orbits with irrationally related frequencies that lead to chaos. The system loses stability through Hopf bifurcations. Assume that a system with a steady state solution loses its stability, as some control parameter is varied, through a Hopf bifurcation (ie. a pair of complex eigenvalues crosses the imaginary axis). The steady state becomes oscillatory. Assume that this happens three times in succession and that the three newly created modes are essentially independent - then chaos may occur. The precursor is the existence of quasi-periodic motions.

The power spectrum will exhibit one, then two, and possibly three independent basic frequencies. When the third frequency is about to appear simultaneously some broad-band noise will appear – this is then regarded as chaotic. Evidence is from Taylor-Couette vortices in fluid flow between rotating cylinders and in Rayleigh-Bnard convection.

## **2.4 A statistical description of chaos**

The previous examples suggest that trajectories of maps and dynamical systems are predictable when orbits are fixed points or periodic oscillations. After the onset of chaos, instead, there seem to be little hope to predict the details of the trajectories. This situation is similar to what happens in the study of fluid flows. When the Reynolds number is small, solutions are linear and predictable. At large Reynolds

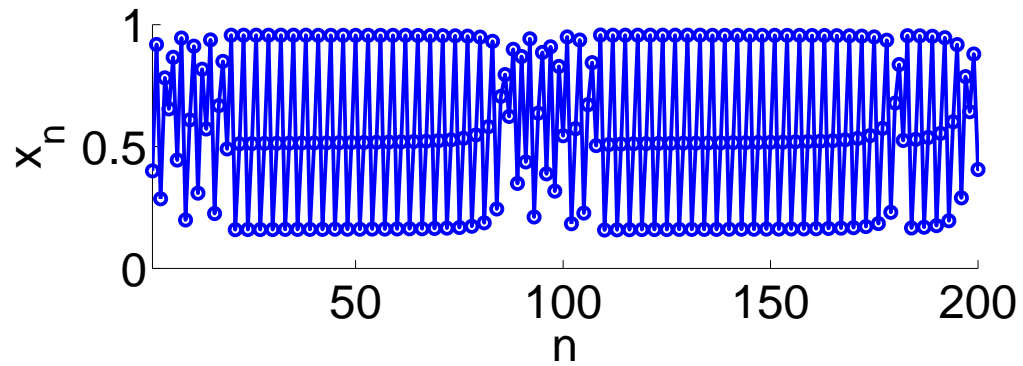


Figure 2.3: Intermittency route to chaos in the logistic map for  $r = 3.8282$ . Part of the orbit looks like a stable period three cycle, as indicated by the blue circles. But this is spooky since the period three orbit no longer exists! We are seeing the ghost of the three cycle.

numbers, the flow becomes erratic and exact solutions cannot be found neither analytically, nor numerically. Does it mean that a theory of turbulence is beyond our reach?

Let us consider the logistic map with  $r = 4$ , in the strongly chaotic regime. The map displays broadband spectrum in time, nonlinearity, unpredictable behavior, and time irreversibility (Fig. 2.4). However the histogram of the positions  $x$  assumed by the orbit is quite predictable (Fig. 2.4). In the chaotic regime the histograms show a predictability that does not emerge in individual trajectories. The histogram always converge toward the same distribution, regardless of initial conditions. Why does the histogram of the logistic map converge to a limit solution? Why a deterministic system such as a map has a regular statistical behavior? We do not have complete answers to these equations, but progress is being made. The current understanding is that maps in the chaotic regime collapse on a strange attractor which is a generalization of the fixed points and periodic orbits in the linear regime. The structure of strange attractors is very complex. That is why trajectories are so erratic and difficult to predict. However ensemble of trajectories reflects the mean structure of the attractor and can be predicted.

In this section we derive a statistical description of the logistic map. The goal is to understand the difference between the trajectory-based description and the histogram-based description. First we need to determine the evolution equation for the histogram  $P(v)$ , also known as the probability distribution function, so that we can observe the recurrence relation  $P_{n+1}(v) = UP_n(v)$ . The distribution function  $P_{n+1}(v)$  after  $n + 1$  iterations is obtained by the action of the operator  $U$  on  $P_n(v)$ , which is the distribution function after  $n$  iteration of the map. The operator  $U$  acts on functions and it is known as the Perron-Frobenius operator.

We can derive the Perron-Frobenius operator for the logistic map. We have already shown that by making the change of variables,

$$x_n = \sin^2(\pi z_n/2), \quad (2.29)$$

the logistic map with  $r = 4$  becomes,

$$z_{n+1} = \begin{cases} 2z_n, & 0 \leq z_n \leq 1/2 \\ 2 - 2z_n, & 1/2 \leq z_n \leq 1 \end{cases} \quad (2.30)$$

which is known as the tent map, because of the shape of its graph. We can easily write the Perron-Frobenius operator for the tent map,

$$P_{n+1}(v) = \frac{1}{2} \left[ P_n \left( \frac{v}{2} \right) + P_n \left( 1 - \frac{v}{2} \right) \right]. \quad (2.31)$$

As a consequence of the form of the Perron-Frobenius operator, if  $P_n$  is constant equal to  $P_0$ , then  $P_{n+1}$  is also equal to  $P_0$ . The uniform distribution  $P = P_0$  is

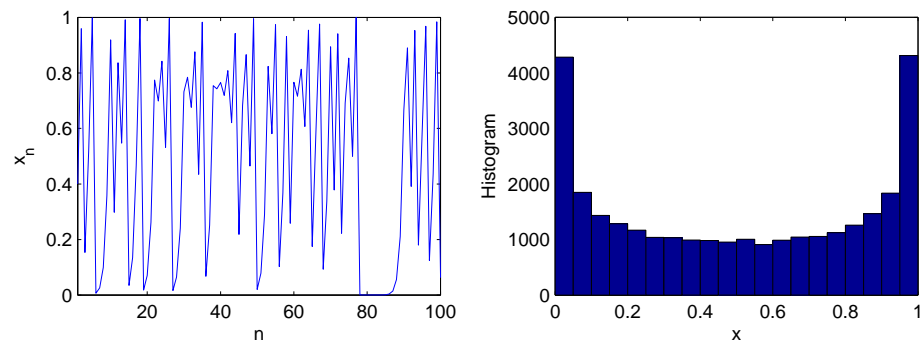


Figure 2.4: A trajectory and the histogram for the logistic map with  $r = 4$ .

the equilibrium distribution. The uniform distribution is indeed the final state that one obtains by running numerical integrations of the tent map. Thus the statistical description predicts a result that cannot be derived from simple inspection of the deterministic equation.

How do we know that the equilibrium distribution is obtained for any set of initial conditions? In order to solve arbitrary initial value problems, we need the full set of eigenfunctions and eigenvalues of the Perron-Frobenius operator. These eigenfunctions can be used to represent any arbitrary initial condition. The eigenfunctions for the tent map belong to a family of polynomials called the *Bernoulli polynomials*. The eigenfunctions are found by solving the problem,

$$P(v) = \lambda UP(v). \quad (2.32)$$

In the example of the tent map, we find that the all eigenfunctions but the uniform distribution have  $\lambda \leq 1$ . For example an eigenfunction is given by,

$$P(v) = v^2 - 2v + \frac{2}{3}. \quad (2.33)$$

This eigenfunction has an eigenvalues  $\lambda = 1/4$ . The uniform distribution  $P = 1$  is the only eigenfunction with eigenvalue  $\lambda = 1$ . Thus all eigenfunctions other than the uniform distribution decay in time. And the uniform distribution emerges as the asymptotic state.

It is left as an exercise to relate the probability distribution of the tent map to that of the poor man's Navier-Stokes map, and show that it correctly predicts what we found by numerical integrations of the map.

## 2.5 Turbulence and chaos

It is finally time to go back to fluid dynamics and try to relate the lessons of chaotic maps to the description of turbulence.

### 2.5.1 Transition to turbulence

#### Lessons from the dynamical system approach

Up to the discovery of chaos in simple deterministic systems, studies on the onset of turbulence dealt with linear and, very rarely, with weakly non-linear evolution of external disturbances. The first physical model of laminar-turbulent transition is due to Landau and it is reported in the fourth volume of the course on Theoretical Physics

(Landau and Lifshitz, 1971). According to this model, as the Reynolds number is increased, the system undergoes an infinite series of Hopf bifurcations. Each bifurcation causes the velocity field to oscillate with a new frequency  $f_i$ , until for sufficiently large  $i$  the motion appears chaotic. In this picture the unpredictability of turbulence arises because each new frequency  $f_i$  is associated with a new phase  $\phi_i$  and, for large  $i$ , it becomes progressively difficult to keep track of all oscillations.

The Landau transition scenario is, however, untenable because a few incommensurate frequencies do not generate positive Lyapunov exponents. And the sensitive dependence on initial conditions is a trademark of turbulent flows. This characteristic feature is now known as the butterfly effect. Thus the transition to turbulence is probably best understood in terms of the routes to chaos observed in maps and simple dynamical systems.

### Shortcomings of the dynamical system approach

Should we then conclude that the onset of turbulence is analogous to the onset of chaos? Unfortunately the story is more complicated. Dynamical systems arise from the projections of the full Navier-Stokes dynamics on a very limited number of spatial scales. The onset of chaos in those systems is then forced to remain confined to few spatial scales. Experiments suggest that the onset of turbulence in real flows is associated with broadband spectra both in time and in space. It is very difficult to set up experiments where there is transition to chaos with the appearance of a broadband spectrum in time, without an increase in the number of the spatial degrees of freedom. Only by carefully designing experiments in closed environments, can one observe the routes to chaos described above in real flows. For the moment, we must conclude that the theory of dynamical systems and chaos provides useful insights in the world of turbulence, but it is not the whole story. We will return to this issue in the discussion of turbulent convection.

## 2.5.2 Statistical description of turbulence

The logistic map is a useful tool to illustrate some important characteristics of turbulent flows. However it is pathological in at least two ways,

- The logistic map explores the full available space  $[0, 1]$ . Typically turbulent systems are dissipative and collapse on an attractor with fractal structure (at least for finite-dimensional systems). This limitation can be overcome considering two dimensional maps.
- Natural systems tend to have more than one attractor. Thus the equilibrium statistical properties are not fully predictable.

Furthermore there are technical issues that have not been solved for the Navier-Stokes equations. We do not know if solutions exist for all times for arbitrary initial condition. We do not know how to write the equivalent of the Perron-Frobenius operator.

Further reading:

Frisch, chapter 1-3

Strogatz, chapter 10

Tritton, chapter 24